Proceedings of the 9th International Scientific and Technical Conference "New Methods and Technologies in Petroleum Geology, Drilling and Reservoir Engineering," Volume II, 311-317, AGH, Krakow, Poland, July 2-3, 1998

CONTROL OF FLUID INJECTION INTO A LOW-PERMEABILITY ROCK - HYDROFRACTURE GROWTH

Tad W. Patzek and Dmitriy B. Silin

Abstract: Injection hydrofractures grow in transient linear flow in a low permeability, soft rock. The cumulative injection of water or steam scales with time to the power of 1, not ½ predicted from the theory of linear transient flow. Therefore, either the injection hydrofractures grow with time, or the formation permeability increases with time, or both. A simple mass balance of hydrofracture growth during fluid injection, attributed to Carter, is corrected, extended to the case of variable injection pressure, and presented in a simplified form. The Carter theory predictions are then compared with the growth rate of hydrofracture area calculated independently for two steam injectors. There is remarkable agreement between the modified Carter theory predictions and the independently estimated rates of growth of these two hydrofractures.

Department of Materials Science and Mineral Engineering, University of California, Berkeley, Berkeley, CA 94720, 011-510-643-5834, Fax 011-510-642-3805, patzek@patzek.berkeley.edu

1. Introduction: Field demonstrations of hydrofracture propagation and geometry are scarce. Kuo *et al.* [1] proposed a fracture extension mechanism to explain daily wellhead injection pressure behavior observed in the Stomatito Field A fault block in the Talara Area of the Northwest Peru. They have quantified the periodic increases in injection pressure, followed by abrupt decreases, in terms of Carter's theory [2] of hydrofracture extension. Patzek [3] described several examples of injector-producer hydrofracture linkage in the South Belridge diatomite, CA, and quantified the discrete extensions of injection hydrofractures using the linear transient flow theory and linear superposition method.

Vinegar *et al.* [4] used three remote "listening" wells with multiple cemented geophones to triangulate the microseismic events during hydrofracturing of a well in a steam drive pilot in Section 29 of the South Belridge diatomite. Ilederon *et al.* [5] used the same geophone array to triangulate microseismicity during hydrofracturing of two steam injectors nearby. In addition, they corrected the triangulation for azimuthal heterogeneity of the rock by using conical waves. Multiple fractured intervals, each with very different lengths of hydrofracture wings, as well as an unsymmetrical hydrofracture, have been reported.

To date, perhaps the most complete images of hydrofracture shape and growth rate *in situ* have been presented by Kovscek *et al.* [6, 7]. They have obtained detailed time-lapse images of two injection hydrofractures in the South Belridge diatomite, Section 29, Phase II steam drive pilot.

This paper is organized as follows. First, Carter's theory[2] of fracture growth is revisited and extended to the case of variable injection pressure. Carter's assumptions are clarified and corrected. A new, simple expression is obtained for the cumulative fluid injection as a function of variable injection pressure and fracture area. Fracture growth is expressed in terms of readily available field measurements. Second, for a steam injector in the South Belridge diatomite, predictions of the modified [8] Carter theory are compared with the hydrofracture growth calculated independently by Kovscek *et al.* [6, 7].

2. Carter's Model Revisited: Let us formulate a one-dimensional model of fluid injection from a vertical highly conductive fracture into a low-permeability rock. We assume to know the entire history of variable injection pressure, the initial fracture area - not necessarily zero, and the entire history of fracture growth. We also assume that the flow of the injected incompressible fluid is horizontal, transient, and perpendicular to the fracture plane. Thus the injection pressure is not communicated beyond the current length of the fracture, and the injection well is in an infinite reservoir. We denote by $A(t)$ and $dA(t)/dt$, respectively, the fracture area and the rate of fracture growth at time *t*; hence the initial fracture area is $A(0)$. We denote by $q(t)$ and $p_{inj}(t)$ the injection rate and the average downhole injection pressure, respectively. We assume that the permeability inside the fracture is much higher than in the surrounding formation; therefore, at each time the fluid pressure is essentially the same throughout the fracture.

Now let us pick an arbitrary time τ between 0 and t. We define $v_{\tau+\varepsilon\Delta\tau}(t)$, $0<\varepsilon<1$, as the fluid superficial leak-off velocity at time t across that portion of the fracture which opened between τ and $\tau+\Delta\tau$, $\Delta\tau$ being a small increment of time. The new fracture area, which has been created within the time interval $[\tau,\ \tau+\Delta\tau]$, is equal to $A(\tau+\Delta\tau)-A(\tau)$. Hence the rate of fluid leak-off through this area is equal to $\Delta q_\tau(t)=2v_{\tau+\varepsilon\Delta\tau}(t)\big(A(\tau+\Delta\tau)-A(\tau)\big)$. The coefficient of 2 is implied by the assumption that the fracture is two-sided and the fluid leaks symmetrically into the formation. The rate of leak-off from the originally open fracture area is $q_0(t)=2v_0(t)A(0)$. Let us split the time interval $[0,t]$ by a partition $\{0=\tau_0<\tau_1<\ldots<\tau_K=t\}$ into small contiguous non-overlapping subintervals $[\tau_k,\ \tau_k+\Delta\tau_k]$, $\Delta\tau_k=\tau_{k+1}-\tau_k$ and apply the above calculations to each subinterval. Summing up over all intervals $[\tau_k,\ \tau_k+\Delta\tau_k]$ and adding $w dA(t)/dt$, the rate of water accumulation from fracture extension, one gets:

$$\begin{aligned}
&q(t)=q_0(t)+\Delta q_0(t)+\Delta q_1(t)+\ldots+\Delta q_{K-1}(t)+w\frac{dA}{dt}=2v_0(t)A(0)+\\
&2v_{\tau_0+\varepsilon_0\Delta\tau_0}(t)\big(A(\tau_0+\Delta\tau_0)-A(\tau_0)\big)+2v_{\tau_1+\varepsilon_1\Delta\tau_1}(t)\big(A(\tau_1+\Delta\tau_1)-A(\tau_1)\big)+\\
&2v_{\tau_{K-1}+\varepsilon_{K-1}\Delta\tau_{K-1}}(t)\big(A(\tau_{K-1}+\Delta\tau_{K-1})-A(\tau_{K-1})\big)+w\frac{dA}{dt}.
\end{aligned}\tag{1}$$

Here w is the average fracture width. Passing to the limit as $\max\limits_k(\Delta\tau_k)\to 0$, we obtain

$$q(t)=2v_0(t)A(0)+2\int_0^t v_\tau(t)\frac{dA(\tau)}{d\tau}\,d\tau+w\frac{dA(t)}{dt}.\tag{2}$$

Remark. Strictly speaking, the above calculations should yield a single Riemann-Stieltjes integral [9]: $2\int_0^t v_\tau(t)\ dA(\tau)$ for the first two terms in (2). In this case, $A(t)$ plays the role of a measure defined on $t \geq 0$. However, here we assume that $A(t)$ is at least absolutely continuous on $[0,+\infty)$ and use Eq. (2) with the explicit initial fracture area of $A(0)$. This is a relatively mild restriction because we can always approximate a non-smooth model with a smooth one.

If the injection pressure is constant, then the leak-off velocity $v_\tau(t)$ depends only on the difference $t-\tau$, i.e., on how long ago from the present the respective portion of the fracture opened. Thus we can substitute $v_\tau(t) = v(t-\tau)$ into (2):

$$q(t) = 2v_0(t)A(0) + 2\int_0^t v(t-\tau)\frac{dA(\tau)}{d\tau}\ d\tau + w\frac{dA(t)}{dt}. \tag{3}$$

Eq. (3) extends the original Carter model[2] of fracture growth by accounting for the initial fracture area $A(0)$.

Now let us find out how $v_\tau(t)$ depends on $p_{inj}(t)$ if the injection pressure varies with time. For this purpose, we consider the following parabolic boundary-value problem on a semi-infinite interval:

$$\begin{aligned} &\frac{\partial p_\tau}{\partial t} = \alpha\frac{\partial^2 p_\tau}{\partial x^2}, \quad t \geq \tau, \quad x \geq 0, \\ &p_\tau(x,\tau) = \begin{cases} p_{inj}(\tau), & x = 0, \\ p_i, & x > 0, \end{cases} \qquad p_\tau(0,t) = p_{inj}(t). \end{aligned} \tag{4}$$

Here α and p_i denote, respectively, the constant hydraulic diffusivity and the initial pressure in the formation outside the fracture area created at time τ. The solution to the boundary-value problem (4) characterizes the distribution of pressure outside the fracture caused by fluid injection: $p_\tau(x,t)$ is equal to the pressure at time t at a point located at the distance x from the portion of the fracture, which opened at time τ. According to Darcy's law,

$$v_\tau(t) = -\frac{kk_r}{\mu}\frac{\partial p_\tau(0,t)}{\partial x}. \tag{5}$$

Here k and k_r are the absolute rock permeability and the relative fluid permeability in the formation outside the fracture, and μ is the fluid viscosity.

The solution to the boundary value problem (4) is known (cf. [10] or [11]):

$$p_\tau(x,t) = p_i + \frac{2}{\sqrt{\pi}}\int_{\frac{x}{2\sqrt{\alpha(t-\tau)}}}^{\infty}\left[p_{inj}\left(t - \frac{x^2}{4\alpha\xi^2}\right) - p_i\right]e^{-\xi^2}d\xi, \quad t \geq \tau, \quad x \geq 0, \tag{6}$$

It can be shown that

$$\left.\frac{\partial p_\tau(x,t)}{\partial x}\right|_{x=+0}=-\left(\frac{1}{\sqrt{\pi\alpha(t-\tau)}}\left[p_{inj}(\tau)-p_i\right]+\frac{1}{\sqrt{\pi\alpha}}\int_\tau^t\frac{p'_{inj}(\xi)}{\sqrt{t-\xi}}d\xi\right). \tag{7}$$

Substitution into (5) yields

$$v_\tau(t)=\frac{kk_r}{\mu}\left(\frac{1}{\sqrt{\pi\alpha(t-\tau)}}\left[p_{inj}(\tau)-p_i\right]+\frac{1}{\sqrt{\pi\alpha}}\int_\tau^t\frac{p'_{inj}(\xi)}{\sqrt{t-\xi}}d\xi\right) \tag{8}$$

Now it only remains to substitute (8) into (3), take into account that $p_{inj}(t)=p_{inj}(0)+\int_0^\tau p'_{inj}(\tau)\,d\tau$, and change the order of iterated integration:

$$\begin{aligned}q(t)=w\frac{dA(t)}{dt}&+2\frac{kk_r}{\mu\sqrt{\pi\alpha}}\left(p_{inj}(0)-p_i\right)\left(\frac{A(0)}{\sqrt{t}}+\int_0^t\frac{1}{\sqrt{t-\xi}}\frac{dA(\xi)}{d\xi}d\xi\right)+\\ 2\frac{kk_r}{\mu\sqrt{\pi\alpha}}&\int_0^t p'_{inj}(\tau)\left(\frac{A(\tau)}{\sqrt{t-\tau}}+\int_\tau^t\frac{1}{\sqrt{t-\xi}}\frac{dA(\xi)}{d\xi}d\xi\right)d\tau.\end{aligned} \tag{9}$$

Eq. (9) may be integrated with respect to time and simplified to

$$Q(t)=wA(t)+2\frac{kk_r}{\mu\sqrt{\pi\alpha}}\int_0^t\frac{\left(p_{inj}(\tau)-p_i\right)A(\tau)}{\sqrt{t-\tau}}d\tau\ , \tag{10}$$

where $Q(t)=\int_0^t q(\tau)d\tau$ is the cumulative injection at time t .

Eq.(10) is the most general model of fluid injection as a function of injection pressure and fracture area, and under the assumptions listed above. To our knowledge, such an equation has not been published elsewhere. In particular, it implies the following special cases.

(1) If there is no fracture growth and injection pressure is constant, i.e., $A(t)\equiv A_0$ and $p_{inj}(t)\equiv p_{inj}$, then

$$Q(t)=wA_0+4A_0\frac{kk_r}{\mu\sqrt{\pi\alpha}}\left(p_{inj}-p_i\right)\sqrt{t}\ . \tag{11}$$

and injection rate must decrease inversely proportionally to the square root of time:

$$q(t)=2\frac{kk_r}{\mu\sqrt{\pi\alpha}}\left(p_{inj}-p_i\right)\frac{A_0}{\sqrt{t}} \tag{12}$$

The leak-off velocity is

$$v(t) = \frac{q(t)}{2A_0} = \frac{kk_r}{\mu}\frac{\left(p_{inj} - p_i\right)}{\sqrt{\pi\alpha t}} = \frac{C}{\sqrt{t}}, \quad \text{where } C = \frac{kk_r}{\mu}\frac{\left(p_{inj} - p_i\right)}{\sqrt{\pi\alpha}}. \tag{13}$$

The cumulative fluid injection can be expressed through C:

$$Q(t) - wA_0 = 4A_0\frac{kk_r}{\mu}\frac{\left(p_{inj} - p_i\right)}{\sqrt{\pi\alpha}}\sqrt{t} = 4A_0C\sqrt{t} = (\text{Early Injection Slope})\sqrt{t}, \tag{14}$$

where the "Early Injection Slope" characterizes fluid injection prior to fracture growth and prior to changes in injection pressure. Note that if *v* is in *ft/day*, then *C* is in $ft/\sqrt{day}$, and from (14) it follows that

$$C = \frac{1}{4A_0}\left(1.127\times 10^{-3} \times \text{Early injection slope, BCWE}/\sqrt{\text{Day}}\right). \tag{15}$$

(2) If the cumulative injection and injection rate are, respectively, equal to

$$Q(t) = wA_0 + 4\frac{kk_r}{\mu\sqrt{\pi\alpha}}\left(p_{inj} - p_i\right)A_0\sqrt{t} + q_0 t \tag{16}$$

and

$$q(t) = 2\frac{kk_w}{\mu\sqrt{\pi\alpha}\sqrt{t}}\left(p_{inj} - p_i\right)A_0 + q_0, \tag{17}$$

then the solution to (3) with respect to $A(t)$ is provided by

$$A(t) = A_0 + \frac{q_0 w}{4\pi C^2}\left[e^{\tau_D}\operatorname{erfc}\left(\sqrt{\tau_D}\right) + \frac{2}{\sqrt{\pi}}\sqrt{\tau_D} - 1\right], \tag{18}$$

where

$$\tau_D = \frac{4\pi C^2}{w^2}t = \frac{\pi}{4}\left(\frac{\text{Early Injection Slope}}{\text{Initial Fracture Volume}}\right)^2 t \tag{19}$$

is the dimensionless drainage time of the initial fracture, and wA_0 is the correct spurt loss from the instantaneous creation of fracture at $t = 0$ and filling it with fluid. The formula (17) for the injection rate consists of two parts: the first component is the leak-off rate when there is no fracture extension and the second, constant, component is "spent" on fracture growth. Conversely, the first constant term in the solution (18) is produced by the first term in (17) and the second additive term is produced by the constant component q_0 of $q(t)$ in (17).

For longer injection times $q(t) \approx q_0$, and it can be shown that

$$A(t) \approx A_0\left(1 + \frac{q_0}{\pi C A_0}\sqrt{t}\right) = A_0\left(1 + \frac{4q_0}{\pi\ \text{Early Injection Slope}}\sqrt{t}\right), \tag{20}$$

where the average fluid injection rate q_0 and the Early Injection Slope are in consistent units. For short injection times, the hydrofracture area grows linearly with time (e.g., [12], page 174).

Eq. (20) allows one to calculate the fracture area as a function of average injection rate and the early slope of cumulative injection versus the square root of time. All of these parameters are readily available if one operates a new injection well at a low and constant injection pressure to prevent fracture extension. The initial fracture area (i.e., its length and height) is known approximately from the design of the hydrofracturing job [13, 14].

The most important restriction in Carter's and our derivation is the requirement that the injection pressure is not communicated beyond the current length of the fracture. Hagoort *et al*. have shown numerically [8] that for a homogeneous reservoir the fracture propagation rate is only about half of that predicted by the Carter formula (3). This is because the formation pressure increases beyond the current length of the hydrofracture, thus confining it. If fracture growth is slower than predicted by the mass balance (20), then there must be flow parallel [8] to the fracture plane or additional formation fracturing perpendicular to the fracture plane, or both. Either way, the leak-off rate from the fracture must increase.

3. Injection Fractures Extend: Fig. 1 demonstrates that the plot of the cumulative steam injection versus the square root of time on injection deviates from a straight line for the South Belridge Diatomite steam injector IN2U. The deviation is positive, and the measured constant steam injection rate exceeds that predicted from the theory of transient linear flow of water, Eq. (17). From such observations, one concludes that either the hydrofracture area grows with time, or permeability increases with time, or both.

Fig. 2 plots Eq. (20) with the parameters determined from the field data over a period of roughly 7 years. The predicted hydrofracture extensions vary from a factor of 2.5 for the average waterflood injector in Section 12 of Middle Belridge to a factor of 3.5-5.5 for the three steam injectors in Section 29 of South Belridge. Of course, IN2U and IN2L injected for only 4 years, so they never experienced such large fracture extensions. There is a factor of 1/2 in front of the square root of time in Eq. (20) to account for the reservoir homogeneity perpendicular and parallel to the hydrofracture plane.

Clearly, Fig. 2 predicts very large fracture extensions, and these predictions must be verified by an independent experiment. Luckily, an independent interpretation of hydrofracture geometry in the Phase II steam drive pilot [6, 7] provides the necessary verification. The latter interpretation lumps the parameters that describe the first-order physics of steam flow in diatomite into a single parameter, called the hydraulic diffusivity. This lumping led to a second-order partial differential equation, similar in form to a transient diffusion equation that describes the pressure profile in the steam-occupied zone in each diatomite layer. The method of Marx and Langenheim [15] was then used to locate the steam front in each layer. Finally the transient heat conduction equation was solved for the temperature in the oil zone ahead of the steam front. The hydraulic and thermal diffusivities as well as hydrofracture shape were iterated to match the areal temperature response in each layer of the South Belridge diatomite in the Phase II pilot and the overall cumulative steam injection. The hydrofracture shapes obtained from that analysis are shown in **Fig 3**. There are several fracture extensions lumped into discrete events. In other words, each hydrofracture shape is assumed to persist over a period of time listed below it. In reality, the hydrofracture extensions occur continuously for most of the time. The hydrofracture shapes in Figs 3 have been integrated, and the corresponding surface areas are plotted in **Fig. 4** versus the square root of time, together with the predictions from Carter's theory modified for the homogeneous reservoir. Agreement between the theory and field data is remarkable.

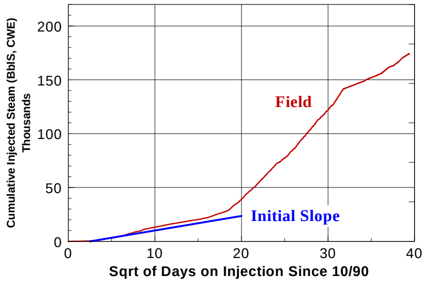

Fig. 1. - Cumulative steam injection in IN2U, Phase II Steam Drive Pilot, Section 29, South Belridge diatomite, CalResources. Note a large positive deviation from the initial injection slope

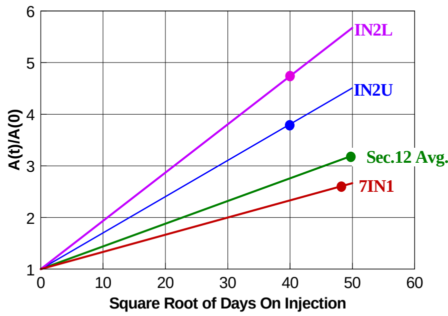

Fig. 2 - Relative extensions of the hydrofracture areas for a homogeneous reservoir. The predictions are 50% of those based on Carter's theory and are in agreement with the simulations by Hagoort *et al*. Note that after 900 days, the hydrofracture in IN2U extends roughly by a factor of 3.

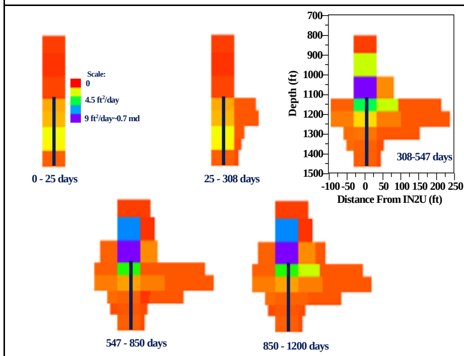

Fig. 3 - Side view of the west face of IN2U hydrofracture and hydraulic diffusivities from history matching. (from *In-Situ* **20**(3), Figure 3A and 3B, pp. 294-295, 1996).

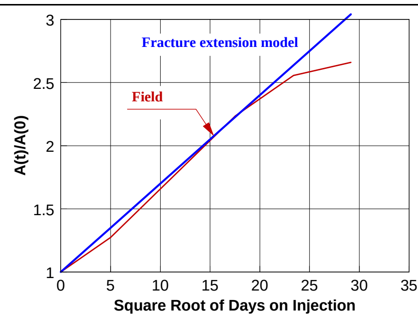

Fig. 4 - Growth of the hydrofracture area in IN2U. The discrete extensions are assumed to have occurred at the beginning of each time interval shown in Fig.12. The homogeneous reservoir prediction agrees very well with the independently obtained hydrofracture areas. Note that at early injection times, the hydrofracture grows linearly with time.

4. Conclusions:

1. We have corrected Carter's transient mass balance of fluid injection through a growing fracture and extended it to the case of variable injection pressure.
2. We have integrated the extended Carter formula with respect to time and presented it in a new simplified form.
3. We have shown that, ultimately, fracture growth is inevitable, regardless of mechanical design of injection wells and injection policy. However, better control of injection pressure through improved mechanical design is always helpful.

4. Hydrofracture extensions manifested themselves as constant injection rates at constant injection pressures.
5. The magnitude of hydrofracture extension can be predicted over a 4-7 year time period from the initial slope of cumulative injection versus the square root of time, average injection rate, and by assuming a homogeneous reservoir.
6. The hydrofracture areas may extend by a factor of 2.5-5.5 after 7 years of water or steam injection.
7. For two steam injectors in the South Belridge diatomite, the hydrofracture growth predictions from the modified Carter theory were found in excellent agreement with their growth rates calculated independently by Kovscek *et al*.

5. References:

1.Kuo, M.C.T., Hanson, H. G., and DesBrisay, C. L. *Paper SPE 12769, Prediction of Fracture Extension During Waterflood*. in *1984 California Regional Meeting*. 1984. Long Beach: SPE.
2.Carter, R.D., *Derivation of the General Equation for Estimating the Extent of the Fractured Area.* Drill. and Prod. Prac., API, 1957: p. 261-268.
3.Patzek, T.W., *Paper SPE 24040, Surveillance of South Belridge Diatomite*. in *SPE Western Regional Meeting*. 1992. Bakersfield: SPE.
4.Vinegar, H.J., et al., *Active and Passive Seismic Imaging of a Hydraulic fracture in the Diatomite.* JPT, 1992. **44**(January): p. 28.
5.Ilderton, D., Patzek, T. E., Rector, J. W., and Vinegar, H. J., *Microseismic Imaging of Hydrofractures in the Diatomite.* SPE Formation Evaluation, 1996(March): p. 46-54.
6.Kovscek, A.R., Johnston, R. M., and Patzek, T.W., *Interpretation of Hydrofracture Geometry During Steam Injection Using Temperature Transients, II. Asymmetric Hydrofractures.* In Situ, 1996. **20**(3): p. 289-309.
7.Kovscek, A.R., Johnston, R. M., and Patzek, T.W., *Interpretation of Hydrofracture Geometry During Steam Injection Using Temperature Transients, I. Model Validation.* In Situ, 1996. **20**(3): p. 251-289.
8.Hagoort, J., Weatherill, B. D., and Settari, A., *Modeling the Propagation of Waterflood-Induced Hydraulic Fractures.* SPEJ, 1980(August): p. 293-303.
9.Natanson, I.P., *Theory of functions of a real variable*. 1955, New York: Ungar Pub. Co.
10.Carslaw, J.C., and Jaeger, J. C., *Conduction of Heat in Solids*. 2 ed. 1959: Clarendon Press, Oxford.
11.Tikhonov, A.N., and Samarskii, A. A., *Equations of mathematical physics*. International series of monographs in pure and applied mathematics; v. 39. 1963, New York: Macmillan.
12.Valko, P., and Economides, M. J., *Hydraulic Fracture Mechanics*. 1995, New York: John Wiley & Sons, Inc.
13.Shlapobersky, J., Walhaug, W. W., Sheffield, R. E., and Huckabee, P. T. *SPE 18195, Field Determination of Fracturing Parameters for Overpressure Calibrated Design of Hydraulic Fracturing*. in *63rd Annual Technical Conference and Exhibition of the SPE*. 1988. Houston, TX: SPE.
14.Shlapobersky, J., Walhaug, W. W. *SPE 18194, Overpressure Calibrated Design of Hydraulic Fracture Stimulations*. in *63rd Annual Technical Conference and Exhibition of the SPE*. 1988. Houston, TX: SPE.
15.Marx, J.W., and Langenheim, R. H., *Reservoir Heating by Hot Fluid Injection.* Trans. AIME, 1959. **216**: p. 312-215.